DOI: 10.1002/chem.201203255

meso-Thiaporphyrinoids Revisited: Missing of Sulfur by Small Metals

Hiroki Kamiya, Takeshi Kondo, Takafumi Sakida, Shigeru Yamaguchi, and Hiroshi Shinokubo*[a]

Abstract: Facile synthesis of *meso*-aryl-substituted 5,15-dithiaporphyrins and 10-thiacorroles has been achieved by sulfidation of α,α′-dichlorodipyrrin metal complexes with sodium sulfide in DMF. Thiacorrole metal complexes exhibit distinct aromaticity due to 18π-conjugation including the lone pair on sulfur, whereas dithiaporphyrins are nonaromatic judging from ^{1}H NMR spectra, X-ray analysis, and absorption spectra. We have found that Ni^{II} and Al^{III} dithiaporphyrin complexes undergo smooth thermal sulfur extrusion reaction to give the corresponding thiacorrole complexes, whereas free base, Zn^{II}, Pd^{II}, and Pt^{II} dithiaporphyrin complexes did not exhibit the similar reactivity. The DFT calculations have elucidated a reaction pathway involving an episulfide intermediate, which can explain the markedly different reactivity among dithiaporphyrin metal complexes.

Keywords: aromaticity · C–C bond formation · nickel · porphyrinoids · sulfur

Introduction

Porphyrins, pyrrole NH of which is replaced with a chalcogen atom, namely, core-modified porphyrins, have attracted considerable attention due to their remarkable properties (Scheme 1).[1,2] This modification significantly changes structural, photophysical, and electronic features, as well as coordination behavior at the central cavity.[3] In addition, expanded core-modified porphyrins were reported to have extremely large two photon cross-sections.[4,5] However, in core-modified porphyrins, the chalcogen atom does not directly participate in the macrocyclic conjugation pathway, but rather acts as a substituent to the normal porphyrinic π system.

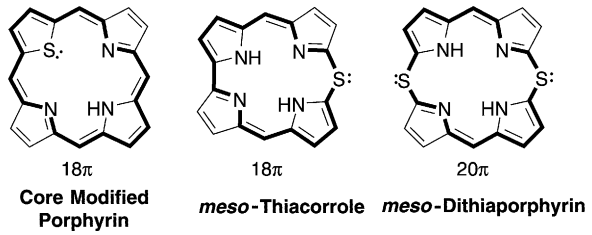

Scheme 1. Structures of representative thiaporphyrinoids. Core-modified porphyrin (21-thiaporphyrin), 10-thiacorrole, and 5,15-dithiaporphyrin. The bold lines indicate the cyclic π conjugation.

In contrast to core modifications, *meso*-modified porphyrins have heteroatoms directly on the π-conjugation circuit (Scheme 1), and consequently the heteroatom substitution at the *meso*-positions should have significant impact to their electronic structures. In particular, incorporation of 3p or higher atomic orbitals on the heteroatom in the macrocyclic π-conjugated system would lead to intriguing features.

In 1972, for *meso*-dithiaporphyrins, Broadhurst, Grigg, and Johnson reported the synthesis of octaalkyl-5,15-dithiaporphyrin from dipyrrolyl sulfide precursors (Scheme 2).[6,7] They also reported a unique sulfur extrusion reaction of 5,15-dithiaporphyrin to 10-thiacorroles at very high temperature in the presence of triphenylphosphine. However, after this pioneering work, these systems have not been explored further, probably due to synthetic difficulties of these *meso*-

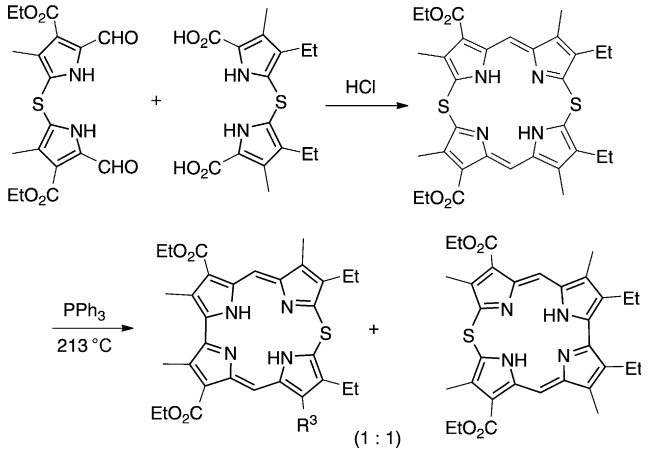

Scheme 2. Formation of 5,15-dithiaporphyrin and 10-thiacorroles from dipyrrolyl sulfides by Grigg et al.

[a] H. Kamiya, T. Kondo, T. Sakida, Dr. S. Yamaguchi, Prof. Dr. H. Shinokubo
Department of Applied Chemistry
Graduate School of Engineering, Nagoya University
Furo-cho, Chikusa-ku, Nagoya, Aichi 464-8603 (Japan)
Fax: (+81) 52-789-5113
E-mail: hshino@apchem.nagoya-u.ac.jp

Supporting information for this article is available on the WWW under http://dx.doi.org/10.1002/chem.201203255.

thiaporphyrinoids.[8] Furthermore, there have been no precedent reports on the synthesis of *meso*-aryl-substituted *meso*-thiaporphyrinoids, nature of which would be finely tuned by the aryl substituents, similar to the case of *meso*-aryl-substituted porphyrins.

Recently, we have established synthesis of Ni^{II} azacorroles from a Ni^{II} dipyrrin complex **1** through Pd-catalyzed Buchwald–Hartwig amination.[9] Meanwhile, Matano et al. have independently developed a highly efficient synthetic procedure for 5,10-diazaporphyrins from dipyrrin metal complexes.[10] We further extended this strategy to preparation of 16π-antiaromatic norcorrole Ni^{II}.[11] We next undertook incorporation of sulfur to the porphyrin skeleton at the *meso*-positions through nucleophilic sulfidation of halogenated dipyrrin precursors **1**. Now we have accomplished a facile metal-templated synthesis of *meso*-aryl-substituted 10-thiacorroles and 5,15-dithiaporphyrins, which allowed detailed investigation on the structures and properties of this intriguing class of old-but-new porphyrinoids.

Results and Discussion

Synthesis and structural characterization: The synthetic protocol of *meso*-thiaporphyrinoids is illustrated in Scheme 3.

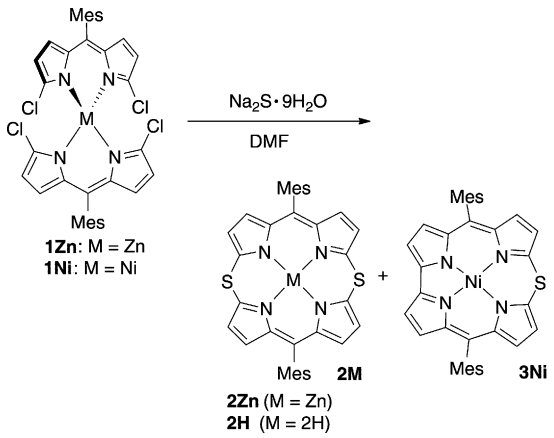

Scheme 3. Sulfidation of α,α′-dichlorodipyrrin complexes **1**.

We found that treatment of α,α′-dichlorodipyrrin Zn^{II} complex **1Zn** with sodium sulfide hydrate in DMF at 65 °C gave 5,15-dithiaporphyrin free base **2H** in 53 % yield along with a small amount of **2Zn**. To investigate the effect of the central metals upon this cyclization reaction, sulfidation of the corresponding Ni^{II} dipyrrin complex **1Ni** was examined under the similar conditions. Surprisingly, 10-thiacorrole Ni^{II} complex **3Ni** was obtained as a sole product in 41 % yield from **1Ni**. None of 5,15-dithiaporphyrin Ni^{II} complex **2Ni** was detected in the reaction mixture.

The structures of these thiaporphyrinoids were unambiguously elucidated by the X-ray crystallographic analysis of Zn^{II} dithiaporphyrin **2Zn** and Ni^{II} thiacorrole **3Ni** (Figure 1). In complex **2Zn**, the two dipyrrin moieties are substantially bent at the sulfur atoms with a dihedral angle of 143.8° (Figure 1b). This folded conformation of the dipyrrin plane is structurally closely related to porphodimethenes.[12] Thus, dithiaporphyrin **2** can be referred to as thia-calix[4]phyrins. One of the sulfur atoms is bound to the zinc center in another molecule of **2Zn** to form a dimeric structure in the solid state (Figure 1e). The zinc atom is also ligated by acetonitrile used for recrystallization.[13] In sharp contrast, thiacorrole Ni^{II} **3Ni** has a highly planar structure with a mean plane deviation of 0.036 Å (Figure 1a and b). Importantly, the carbon–sulfur bond length is 1.69 Å, which is substantially shorter than that in **2Zn** (1.75 Å) and a typical C–S bond length (1.82 Å). The shrunk bond length is due to the partial double bond character of the C–S bond in **3Ni**, indicating effective delocalization of the lone pair on sulfur to the π system.

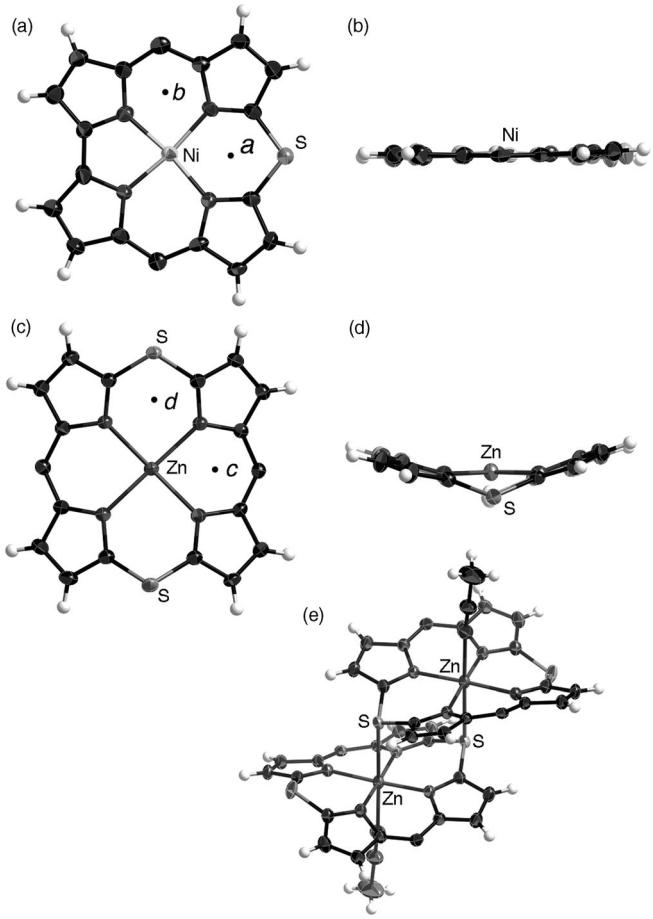

Figure 1. X-ray crystal structures of **3Ni**: a) top view; b) side view and of **2Zn**: c) top view; d) side view; and e) oblique view of the dimeric structure. *meso*-Aryl substituents were omitted for clarity. The thermal ellipsoids were scaled to the 50 % probability level.

Aromaticity of 5,15-dithiaporphyrin and 10-thiacorrole: The ^{1}H NMR spectrum of **3Ni** exhibited four doublet peaks for β-pyrrolic protons in the aromatic region ($\delta = 7.9$–8.4 ppm).

Consequently, thiacorrole Ni^{II} **3Ni** is concluded to be a distinctly aromatic porphyrinoid. To support aromaticity of **3Ni**, the nucleus-independent chemical-shift (NICS) calculations by the DFT method at the B3YP/631SDD level of theory were further performed (631SDD denotes a basis set consisting of SDD for Ni and Zn and 6–31G(d) for the rest).[14] The NICS values at the points "*a*" and "*b*" (indicated in Figure 1a) were calculated to be $\delta = -15.0$ and -11.5 ppm, respectively, supporting strong aromatic character of **3Ni**. The aromaticity of **3Ni** clearly indicates that the lone pair in the 3p orbital on sulfur actually participates in the 18π conjugation as depicted in Scheme 1. Importantly, Grigg et al. reported that *meso*-protons of octaalkyl-10-thiacorroles appeared round $\delta = 10$ ppm.[6] Therefore, both octaalkyl- and *meso*-aryl-10-thiacorroles can be regarded as aromatic [17]thiaannulenes. Only a few examples of large aromatic thiaannulenes with odd numbered rings were reported.[15] In contrast, dithiaporphyrin **2H** and its metal complexes exhibited no significant upfield shift of β-protons in their ^{1}H NMR spectra, thus indicating nonaromatic nature in spite of the potential 20π-electronic system. Due to the substantially bent structure and the long C–S bond, *meso*-dithiaporphyrin can be rather regarded as a sulfur-bridged dipyrrin dimer, lacking in effective global π conjugation over the macrocycle. This situation was again supported by the NICS calculation: the NICS values at the points "*c*" and "*d*" (indicated in Figure 1c) are $\delta = 6.5$ and 2.6 ppm, revealing marginal antiaromaticity of **2Zn**.

Metalation behavior of 5,15-dithiaporphyrin free base: With free base **2H** in hand, metal insertion of **2H** was then examined (Scheme 4). Treatment of **2H** with zinc(II) acetate and nickel(II) acetylacetonate at room temperature successfully gave the corresponding Zn^{II} and Ni^{II} complexes **2Zn** and **2Ni** in excellent yields. Pd^{II} and Pt^{II} complexes **2Pd** and **2Pt** were also obtained from the reaction of **2H** with palladium chloride and platinum chloride. Interestingly, nickel insertion at 110 °C in toluene at reflux gave Ni^{II} thiacorrole **3Ni** in 43 % yield. Furthermore, **2Ni** was converted to **3Ni** in 75 % yield at 100 °C within 2 h in the presence of triphenylphosphine (2.0 equiv) to trap the liberated sulfur atom. Formation of triphenylphosphine sulfide was confirmed by the ^{1}H NMR spectrum of the crude product. Grigg et al. reported that this type of sulfur extrusion occurred at 214 °C in 4.5 h in the case of Zn^{II} octaalkyldithiaporphyrin.[6,16] This may indicate that *meso*-aryl-substituted dithiaporphyrins undergo more facile thermal sulfur extrusion reaction than β-alkyl-substituted ones. Interestingly, no desulfur reaction was observed for **2H**, **2Zn**, **2Pd**, and **2Pt** under the same conditions or at even elevated temperature, namely, at 180 °C. These results strongly suggest the critical role of the central metals in the reactivity of dithiaporphyrin metal complexes.

To examine the origin of the specific reactivity of the nickel complex, structural analysis of **2Ni** was essential. We were pleased to get nice crystals of dithiaporphyrin Ni^{II} and Pt^{II} complexes **2Ni** and **2Pt**. X-ray analysis of these complexes showed that the folding angle of the two dipyrrin planes in **2Ni** is 117.6°, which is much smaller than those in **2Zn** (143.8°) and **2Pt** (134.3°; Figure 2). The average distance of the α-carbons in **2Ni** is 2.64 Å, whereas those in **2Zn** and **2Pt** are 2.79 and 2.71 Å, respectively. On the basis of these different structural factors, we speculated that a smaller metal ion induces more severe bending of the two dipyrrin units in the dithiaporphyrin complex **2**, resulting in a shorter distance between two reacting α-carbons to facili-

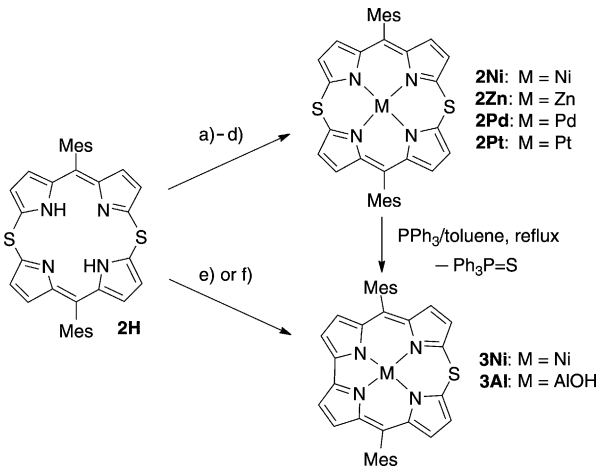

Scheme 4. Metalation of dithiaporphyrin **2H**. Reaction conditions: a) $Ni(acac)_2 \cdot xH_2O$ (10 equiv), CH_2Cl_2, RT, 93 % yield for **2Ni**; b) $Zn(OAc)_2 \cdot 2H_2O$ (10 equiv), CH_2Cl_2, RT, 90 % yield for **2Zn**; c) $PdCl_2$ (5.0 equiv), CH_2Cl_2, RT, 26 % yield for **2Pd**; d) $PtCl_2$ (5.0 equiv), CH_2Cl_2, RT, 14 % yield for **2Pt**; e) $Ni(acac)_2 \cdot xH_2O$ (10 equiv), toluene, 100 °C, 43 % yield for **3Ni**; f) $AlCl_3$ (10 equiv), pyridine, reflux, then PPh_3 (2.0 equiv), toluene, reflux, 73 % yield for **3Al**.

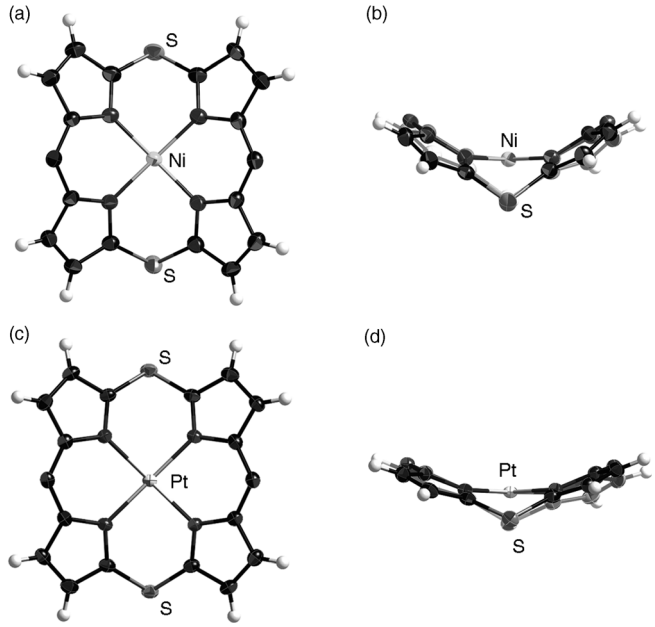

Figure 2. X-ray crystal structures of **2Ni** a) top view; b) side view and of **2Pt**: c) top view and d) side view. *meso*-Aryl substituents are omitted for clarity. The thermal ellipsoids were scaled to the 50 % probability level.

tate carbon–carbon bond formation. To prove this hypothesis, the thermal reactivity of Al^{III} dithiaporphyrin **2Al**, which was prepared from **2H** and $AlCl_3$ in pyridine according to the procedure for insertion of aluminum to regular porphyrins, was checked (Scheme 4 f).[17] To our delight, Al^{III} thiacorrole **3Al** was isolated in 73% yield in two steps from **2H** upon heating the crude Al^{III} complex **2Al**. The ^{1}H NMR spectrum of **3Al** displays all β-pyrrolic protons in the aromatic region, indicating its strong aromaticity of **3Al** as nickel complex **3Ni**.

Reaction mechanism on the basis of DFT calculations: Now we propose the plausible reaction mechanism of the sulfur extrusion reaction, which starts with thermal episulfide formation (Scheme 5). The cyclic array of electrons arising

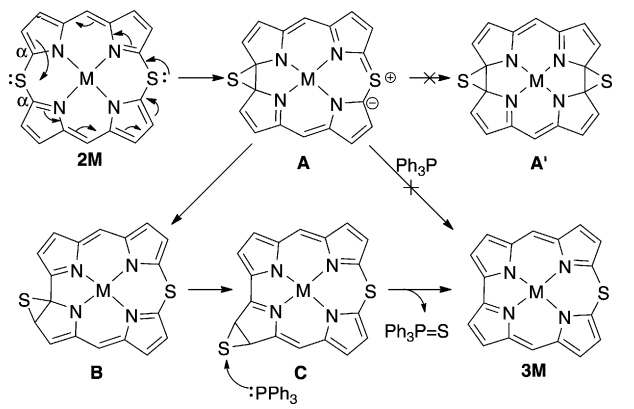

Scheme 5. Proposed reaction mechanism.

from the lone pair on sulfur of **2M** provides the episulfide intermediate **A**, which reasonably explains the critical factor of the folding angle and the distance of the α-carbons. Because of the highly strained structure, involvement of bisepisulfide intermediate **A′** is not likely. The sulfur atom is eventually attacked by triphenylphosphine to afford thiacorrole **3M**.[18,19] Initially we expected that replacement on sulfur of intermediate **A** would directly give **3M**, but we then found that this step is not so straightforward by the DFT calculations.

The reaction mechanism was investigated by computational method with the hope to understand a marked difference in the desulfurization reactivity between **2Ni** and **2Pt**. Initial geometries were obtained from the crystal structures of **2Ni** and **2Pt**. To reduce the calculation cost, two mesityl groups were replaced by hydrogen atoms. The structures were fully optimized with the B3LYP/631SDD level. Zero-point energy and thermal-energy corrections were conducted for all optimized structures. The obtained transition states gave single imaginary frequencies and IRC calculations supported the transition structures.

By gradual reducing the distance between two α-carbons, we could locate the transition state **TS1-Ni**, which was confirmed to lead to episulfide intermediate **A-Ni** by the IRC calculation (Figure 3). The activation energy of this step

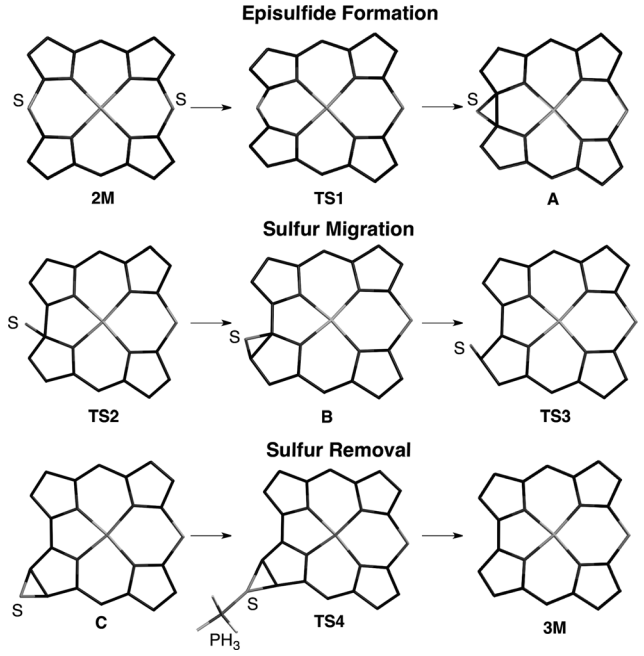

Figure 3. Calculated structures of intermediates and transition states.

from **2Ni** to **TS1-Ni** was calculated to be $E_a = 30.3$ kcal mol^{-1} (Figure 4). We then found that episulfide **A-Ni** underwent facile sulfur migration to 1,2-episulfide **B-Ni** and then 2,3-episulfide **C-Ni** with almost no barriers: the activation energies are only 1.4 and 0.5 kcal mol^{-1}, respectively. The energy of 2,3-episulfide **C** is substantially lower than other intermediates, because **C** should have aromatic stabilization due to retrieval of the 18π-conjugation network. Then phosphine (PH_3) attacks **C**−**Ni** and displaces the sulfur atom to from **3Ni** and phosphine sulfide (PH_3=S). The activation energy of the sulfur removal process was calculated to be

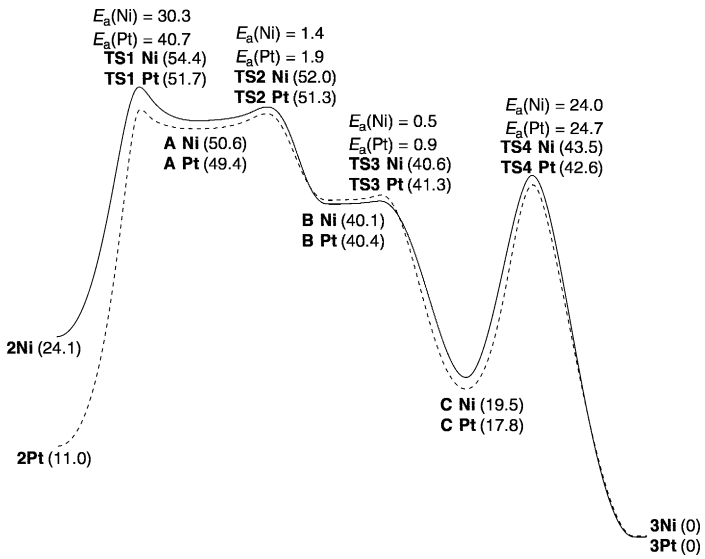

Figure 4. Calculated energy diagrams for sulfur extrusion of **2Ni** and **2Pt** at the B3LYP/631SDD level. The relative energy [kcal mol^{-1}] of each species is shown in parenthesis.

24.0 kcal mol^{-1}. Therefore, the rate-limiting step of the overall sulfur extrusion reaction from **2Ni** to **3Ni** is the formation of the initial episulfide **A−Ni**. Similar intermediates and transition states were also obtained for the corresponding Pt^{II} complexes. The activation energy for the rate-limiting step is 40.7 kcal mol^{-1}, which is substantially higher than that of the nickel complex. Figure 4 shows the energy diagram of the two reaction pathways for **2Ni** and **2Pt**, which indicate relative energies of intermediates and transition states on the basis of the energy levels of the final products **3Ni** and **3Pt**. Obviously, Pt^{II} dithiaporphyrin **2Pt** is more stable than **2Ni**, because **2Pt** lacks distortion due to the bending of the dipyrrin units. Consequently, we concluded that the inherent relative instability of **2Ni** mainly decreases the activation energy of the episulfide formation to facilitate the sulfur extrusion reaction.

Absorption spectra and electrochemistry: In line with distinct aromaticity of 10-thiacorroles observed in their ^{1}H NMR spectra, the UV/Vis absorption spectra of **3Ni** and **3Al** exhibited diagnostic features of aromatic porphyrins including Soret bands and Q bands (Figure 5a). However, the Soret band of **3Ni** is split and the Q-bands are redshifted in comparison to those of **3Al**. This is probably due to interaction of the nickel center with frontier orbitals of the macrocyclic ligand. This scenario was supported by the DFT calculations, which indicated involvement of the d orbital on Ni^{II} in HOMO and decrease of the HOMO–LUMO gap of **3Ni** (Figure S18 in the Supporting Information). The absorption spectrum of Zn^{II} dithiaporphyrin **2Zn** consists of a strong absorption band at $\lambda = 451$ nm and a redshifted weak one at $\lambda = 529$ nm, whereas **2Ni** exhibited a rather broad absorption spectrum (Figure 5b). The absorption property of dithiaporphyrin complexes varies significantly depending on the central metals. These results suggest that the dithiaporphyrin ligand is flexible enough to accommodate various metal ions, inducing the structural change with the bending of the dipyrrin units. This feature is somewhat similar to those observed for calix[4]phyrin metal complexes.

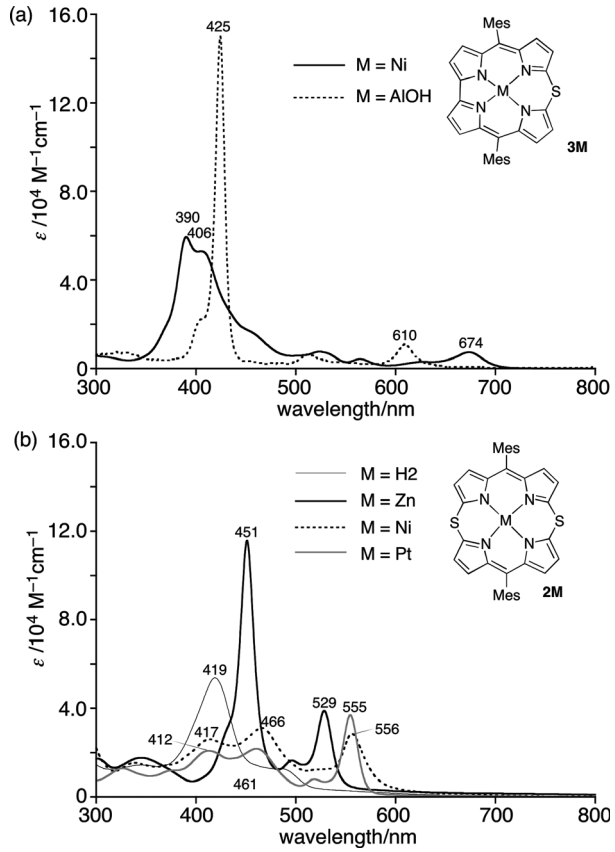

Figure 5. UV/Vis absorption spectra of a) 10-thiacorroles **3M** and b) 5,15-dithiaporphyrins **2M** recorded in CH_2Cl_2.

Electrochemical properties of metal complexes of *meso*-thiaporphyrinoids were investigated by cyclic voltammetry, which was performed in a dichloromethane solution with Bu_4NPF_6 as electrolyte (Figure S16 in the Supporting Information). Two reversible reduction and two reversible oxidation waves were observed, except for **2Zn**. Due to strong electron donation from sulfur to the π system, these thiaporphyrinoids have rather low oxidation potentials. Of them, the first oxidation potential of Zn^{II} dithiaporphyrin **2Zn** was −0.08 V (vs. ferrocene/ferrocenium cation). The differences between the first oxidation and first reduction potentials for **3Ni** and **3Al** are 2.03 and 2.20 V, respectively. The narrower electrochemical HOMO–LUMO gap of **3Ni** than **3Al** is in good agreement with the optical analysis and the DFT calculations.

Conclusion

A facile synthesis of *meso*-aryl-substituted 5,15-dithiaporphyrins and 10-thiacorroles by sulfidation of a bis(α,α′-dichlorodipyrrinato) metal complexes has been achieved. 10-Thiacorrole Ni^{II} and Al^{III} complexes exhibited distinct aromaticity due to 18π electrons including the lone pair on sulfur. In contrast, 5,15-dithiaporphyrins are nonaromatic due to lack of macrocyclic π conjugation. 5,15-Dithiaporphyrin metal complexes showed some similarity to calix[4]phyrins in terms of the folded structure of two dipyrrin units, thus indicating potential utility in molecular-recognition applications. Moreover, the crucial role of the central metals in the sulfur extrusion reaction of dithiaporphyrins to thiacorroles has been elucidated on the basis of X-ray diffraction analysis and DFT calculations. Further investigation of the reactivity and applications of these *meso*-thiaporphyrinoids is currently underway in our laboratory.

Experimental Section

Synthesis of free base dithiaporphyrin 2H: A Schlenk tube containing compound **1Zn** (102 mg, 0.14 mmol) and $Na_2S{\cdot}9H_2O$ (101 mg, 0.42 mmol) was evacuated and then refilled with N_2. Dry DMF (7 mL) was added and mixture was heated at 65 °C for 15 h in oil bath with stirring. After the reaction mixture was cooled to RT, the mixture was passed through a short silica-gel pad (CH_2Cl_2), and the solvent was

evaporated in vacuo. The mixture was purified by silica-gel column chromatography (CH_2Cl_2/hexane) to give **2H** (43.4 mg, 74.2 μmol) in 53% yield as black solid along with a trace amount of **2Zn**. ^{1}H NMR ($CDCl_3$): δ = 2.11 (s, 12H), 2.33 (s, 6H), 6.25 (d, J = 4.0 Hz, 4H), 6.31 (d, J = 4.0 Hz, 4H), 6.90 (s, 4H), 13.00 ppm (s, 2H); ^{13}C NMR ($CDCl_3$): δ = 19.97, 21.07, 120.23, 127.81, 129.18, 133.03, 136.87, 137.63, 138.33, 142.40, and 145.43 ppm; λ_{max} (ε [$M^{-1}cm^{-1}$]) = 419 (5400), 483 nm (1300); HRMS (ESI-MS): m/z calcd for $C_{36}H_{33}N_4S_2^+$: 585.2141 [M+H$^+$]; found: 585.2134.

Synthesis of Zn^{II} dithiaporphyrin 2Zn: A two-necked round bottom flask containing compound **2H** (9.0 mg, 15.4 μmol) and $Zn(OAc)_2 \cdot 2H_2O$ (32.9 mg, 0.15 mmol) was evacuated and then refilled with N_2. To the flask, CH_2Cl_2 (9 mL), methanol (2 mL), and a few drops of Et_3N were added, and mixture was stirring at RT for 12 h. The solvent was evaporated, and the crude material was purified by recrystallization (CH_2Cl_2/methanol) to give **2Zn** (9.0 mg, 13.9 μmol) in 90% yield as red solid. ^{1}H NMR ($CDCl_3$): δ = 2.11 (s, 12H), 2.32 (s, 6H), 6.08 (d, J = 4.0 Hz, 4H), 6.27 (d, J = 4.0 Hz, 4H), 6.86 ppm (s, 4H); ^{13}C NMR ($CDCl_3$): δ = 8.25, 19.98, 21.06, 117.88, 127.58, 131.88, 136.65, 143.99, 150.79 ppm: λ_{max} (ε [$M^{-1}cm^{-1}$]) = 451 (12000), 496 (1600), 529 nm (3900); HRMS (ESI-MS): m/z calcd for $C_{36}H_{30}N_4S_2Zn^+$: 646.1198 [M^+]; found: 646.1180. Crystal data: $C_{38}H_{33}N_5S_2Zn$; M_w = 689.18; monoclinic; space group $P2_1/n$ (No. 14); a = 12.023(5), b = 11.397(5), c = 24.232(5) Å; β = 99.004(5)°; V = 3280(2) Å^3; Z = 4; ρ_{calcd} = 1.396 g cm^{-3}; T = 293(2) K; R = 0.0518 [I > 2.0σ(I)]; R_w = 0.1301 (all data); GOF = 1.045 [I > 2.0σ(I)].[20]

Synthesis of Ni^{II} dithiaporphyrin 2Ni: A two-necked round bottom flask containing compound **2H** (53.0 mg, 90.6 μmol) and $Ni(acac)_2 \cdot xH_2O$ (232 mg, 0.91 mmol) was evacuated and then refilled with N_2. To the flask, CH_2Cl_2 (10 mL) was added, and mixture was stirred at RT for 13 h. The mixture was passed through a short Celite pad (CH_2Cl_2) and evaporated in vacuo without heating. The mixture was purified by recrystallization (CH_2Cl_2/methanol) to give **2Ni** (54.3 mg, 84.6 μmol) in 93% yield as red solid. ^{1}H NMR ($CDCl_3$): δ = 1.85 (s, 6H), 2.33 (s, 6H), 2.45 (s, 6H), 6.16 (d, J = 4.5 Hz, 4H), 6.40 (d, J = 4.5 Hz, 4H), 6.86 (s, 2H), 6.93 ppm (s, 2H); ^{13}C NMR ($CDCl_3$): δ = 19.41, 20.38, 21.08, 117.24, 127.74, 131.56, 132.37, 136.69, 136.91, 137.67, 137.90, 141.13, 150.49 ppm; λ_{max} (ε [$M^{-1}cm^{-1}$]) = 372 (1300), 417 (2300), 466 (3100), 556 nm (2900); HRMS (ESI-MS): m/z calcd for $C_{36}H_{30}N_4S_2Ni^+$: 640.1260 [M^+]; found: 640.1259. Crystal data: $C_{36}H_{30}Cl_{0.25}N_4NiS_2$; M_w = 650.33; triclinic; space group $\bar{P}1$ (No. 2); a = 14.118(4), b = 14.931(4), c = 15.657(4) Å; α = 97.809(4)°, β = 106.390(4)°, γ = 98.193(4)°; V = 3079.7(13) Å^3; Z = 4; ρ_{calcd} = 1.403 g cm^{-3}; T = 293(2) K; R = 0.0447 [I > 2.0σ(I)]; R_w = 0.1232 (all data); GOF = 1.041 [I > 2.0σ(I)].[20]

Synthesis of Pd^{II} dithiaporphyrin 2Pd: A two-neck round bottom flask containing compound **2H** (40.0 mg, 68.4 μmol) and $PdCl_2$ (60.6 mg, 0.34 mmol) was evacuated and then refilled with N_2. To the flask, dry CH_2Cl_2 (0.40 mL) was added, and mixture was stirred at RT for 15 h. The mixture was passed through a short Celite pad (CH_2Cl_2) and evaporated in vacuo. The mixture was purified by silica-gel column chromatography (CH_2Cl_2/hexane) to give **2Pd** (12.4 mg, 18.0 μmol) in 26% yield as red solid. ^{1}H NMR ($CDCl_3$): δ = 2.14 (s, 12H), 2.33 (s, 6H), 6.17 (d, J = 4.5 Hz, 4H), 6.37 (d, J = 4.5 Hz, 4H), 6.89 ppm (s, 4H); ^{13}C NMR ($CDCl_3$): δ = 19.87, 21.08, 116.44, 127.78, 130.80, 133.11, 136.75, 137.39, 137.64, 142.34, 147.40 ppm; λ_{max} (ε [$M^{-1}cm^{-1}$]) = 364 (2200), 464 (5800), 515 (1100), 550 nm (4200); HRMS (ESI-MS): m/z calcd for $C_{36}H_{30}N_4S_2Pd^+$: 608.1539 [M^+]; found: 608.1543.

Synthesis of Pt^{II} dithiaporphyrin 2Pt: A two-neck round bottom flask containing compound **2H** (40.0 mg, 68.4 μmol) and $PtCl_2$ (91.0 mg, 0.34 mmol) was evacuated and then refilled with N_2. To the flask, dry CH_2Cl_2 (0.40 mL) was added and mixture was stirring at RT for 15 h. The mixture was passed through a short Celite pad (CH_2Cl_2) and evaporated in vacuo. The mixture was purified by silica-gel column chromatography (CH_2Cl_2/hexane) to give **2Pt** (7.2 mg, 9.3 μmol) in 14% yield as red solid. ^{1}H NMR ($CDCl_3$): δ = 2.13 (s, 12H), 2.34 (s, 6H), 6.29 (d, J = 4.0 Hz, 4H), 6.45 (d, J = 4.0 Hz, 4H), 6.90 ppm (s, 4H) ppm; ^{13}C NMR ($CDCl_3$): δ = 19.88, 21.09, 115.70, 127.81, 129.86, 132.92, 136.19, 136.79, 137.71, 142.00, 146.77 ppm; λ_{max} (ε [$M^{-1}cm^{-1}$]) = 412 (2100), 461 (2200), 519 (800), 555 nm (3700; HRMS (ESI-MS): m/z calcd for $C_{36}H_{30}N_4S_2Pt^+$: 777.1557 [M^+]; found: 777.1542. Crystal data: $C_{36}H_{29.75}Cl_{0.25}N_4PtS_2$; M_w = 786.46; monoclinic; space group $C2/c$ (No. 15); a = 14.4983(17), b = 14.5316(17), c = 14.8111(17) Å; β = 98.520(2)°; V = 3086.0(6) Å^3; Z = 4; ρ_{calcd} = 1.693 g cm^{-3}; T = 153(2) K; R = 0.0230 [I > 2.0σ(I)]; R_w = 0.0584 (all data); GOF = 1.059 [I > 2.0σ(I)].[20]

Synthesis of Ni^{II} thiacorrole 3Ni: A Schlenk tube containing compound **1Ni** (36.2 mg, 50 μmol) and $Na_2S \cdot 9H_2O$ (24.0 mg, 0.10 mmol) was evacuated and then refilled with N_2. Dry DMF (5 mL) was added, and mixture was stirred at 100 °C for 20 h in oil bath. After cooling the reaction mixture to RT, the mixture was passed through a short silica-gel pad (CH_2Cl_2), and the solvent was evaporated in vacuo. The mixture was purified by silica-gel column chromatography (CH_2Cl_2/hexane) to give **3Ni** (12.6 mg, 20.7 μmol) in 41% yield as black solid. ^{1}H NMR ($CDCl_3$): δ = 1.93 (s, 12H), 2.55 (s, 6H), 7.17 (s, 4H), 7.98 (d, J = 4.5 Hz, 2H), 8.28–8.33 (m, 6H) ppm; ^{13}C NMR ($CDCl_3$): δ = 20.85, 21.34, 117.84, 120.98, 127.46, 127.75, 128.77, 131.53, 133.61, 135.04, 137.51, 137.77, 138.23, 139.76, 146.23 ppm; λ_{max} (ε [$M^{-1}cm^{-1}$]) = 390 (6000), 406 (5300), 524 (760), 564 (420), 627 (300), 674 nm (740); HRMS (ESI-MS): m/z calcd for $C_{36}H_{30}N_4SNi^+$: 608.1539 [M^+]; found: 608.1543. Crystal data: $C_{36}H_{30}N_4NiS$; M_w = 609.41; monoclinic; space group $P2_1/c$ (No. 14).;a = 12.534(14), b = 27.71(3), c = 8.139(9) Å; β = 101.92(2)°; V = 2766(5) Å^3; Z = 4; ρ_{calcd} = 1.463 g cm^{-3}; T = 153(2) K; R = 0.0946 [I > 2.0σ(I)]; R_w = 0.2191 (all data); GOF = 1.242 [I > 2.0σ(I)].[20]

Synthesis of Al^{III} thiacorrole (3Al): A two-neck round bottom flask containing compound **2H** (13.5 mg, 23.1 μmol) and $AlCl_3$ (30.7 mg, 0.231 mmol) was evacuated and then refilled with N_2. Pyridine (5 mL) was added to the flask, and mixture was stirred at reflux for 5 h. The mixture was passed through a short Al_2O_3 pad ($CHCl_3$) and evaporated in vacuo. To the residue, PPh_3 (12.1 mg, 46.2 μmol) and toluene (5 mL) was added, and mixture was heated at refluxed for 12 h. The solvent was evaporated, and the residue was purified by silica-gel column chromatography ($CHCl_3$/methanol). Recrystallization from methanol/H_2O gave **3Al** (10.0 mg, 16.8 μmol) in 73% yield as green solid. ^{1}H NMR ($CDCl_3$): δ = 1.65 (s, 6H), 2.16 (s, 6H), 2.55 (s, 6H), 7.17 (s, 4H), 7.26 (s, 4H), 8.25 (d, J = 4.0 Hz, 2H), 8.40 (d, J = 4.0 Hz, 2H), 8.50 (d, J = 4.0 Hz, 2H), 8.57 ppm (d, J = 4.0 Hz, 2H); ^{13}C NMR ($CDCl_3$): δ = 20.84, 21.61, 21.62, 118.80, 121.00, 128. 08, 128.22, 130.97, 131.17, 131.26, 135.22, 138.14, 138.32, 138.91, 139.11, 141.10, 144.66, 145.21 ppm; λ_{max} (ε [$M^{-1}cm^{-1}$]) = 407 (23000), 425 (150000), 512 (6300), 610 nm (11000); HRMS (ESI-MS): m/z calcd for $C_{36}H_{30}N_4SAl^+$: 577.2001 [M−OH$^+$]; found: 577.1989.

Acknowledgements

This work was supported by Grants-in-Aid for Scientific Research (Nos. 24350023 and 23108705 "pi-Space") from MEXT, Japan. H.S. also acknowledges Daiko Foundation for financial support. S.Y. appreciates the JSPS Research Fellowship for Young Scientists.

[1] For leading reviews on core-modified heteroporphyrins, see: a) L. Latos-Grażyński in *Porphyrin Handbook, Vol. II* (Eds.: K. M. Kadish, K. M. Smith, R. Guilard) Academic Press, San Diego, **2000**, Chapter 14, pp. 361–416; b) P. J. Chmielewski, L. Latos-Grażyński, *Coord. Chem. Rev.* **2005**, *249*, 2510; c) I. Gupta, M. Ravikanth, *Coord. Chem. Rev.* **2006**, *250*, 468; d) A. W. Johnson in *Porphyrins and Metalloporphyrins*, (Ed.: K. M. Smith), Elsevier, Amsterdam, **1975**, Chapter 18, pp. 729–754.

[2] a) A. Ulman, J. Manassen, *J. Am. Chem. Soc.* **1975**, *97*, 6540; b) A. Ulman, J. Manassen, *J. Chem. Soc. Perkin Trans. 1* **1979**, 1066; c) M. J. Broadhurst, A. W. Johnson, R. Grigg, *J. Chem. Soc. C* **1971**, 3681; d) L. Latos-Grazynski, J. Lisowski, M. M. Olmstead, A. L. Balch, *J. Am. Chem. Soc.* **1987**, *109*, 4428; e) W.-S. Cho, H.-J. Kim, B. J. Littler, M. A. Miller, C.-H. Lee, J. S. Lindsey, *J. Org. Chem.* **1999**, *64*, 7890.

[3] For coordination behavior of core-modified porphyrins, see: a) L. Latos-Grażyński, J. Lisowski, P. Chmielewski, M. Grzeszczuk, M. M.

Olmstead, A. L. Balch, *Inorg. Chem.* **1994**, *33*, 192; b) L. Latos-Grażyński, J. Lisowski, M. M. Olmstead, A. L. Balch, *Inorg. Chem.* **1989**, *28*, 1183; c) L. Latos-Grażyński, J. Lisowski, M. M. Olmstead, A. L. Balch, *Inorg. Chem.* **1989**, *28*, 3328; d) C.-H. Chuang, C.-K. Ou, S.-T. Liu, A. Kumar, W.-M. Ching, P.-C. Chiang, M. A. C. de la Rosa, C.-H. Hung, *Inorg. Chem.* **2011**, *50*, 11947.

[4] For reviews on core-modified expanded porphyrins, see: a) T. K. Chandrashekar, S. Venkatraman, *Acc. Chem. Res.* **2003**, *36*, 676; b) R. Misra, T. K. Chandrashekar, *Acc. Chem. Res.* **2008**, *41*, 265.

[5] a) H. Rath, J. Sankar, V. PrabhuRaja, T. K. Chandrashekar, A. Nag, D. Goswami, *J. Am. Chem. Soc.* **2005**, *127*, 11608; b) M.-C. Yoon, R. Misra, Z. S. Yoon, K. S. Kim, J. M. Lim, T. K. Chandrashekar, D. Kim, *J. Phys. Chem. B* **2008**, *112*, 6900.

[6] M. J. Broadhurst, R. Grigg, A. W. Johnson, *J. Chem. Soc. Perkin Trans. 1* **1972**, 1124.

[7] The first synthesis of a 10-thiacorrole complex was achieved by the reaction of a tetrapyrrole palladium(II) complex and sodium sulfide, see: A. W. Johnson, I. T. Kay, R. Rodrigo, *J. Chem. Soc.* **1963**, 2336.

[8] Recently, Bröring et al. have presented synthesis and properties of several metal complexes of octaalkyl-10-thiacorroles at *7th International Conference on Porphyrins and Phthalocyanines*, Korea, **2012**.

[9] M. Horie, Y. Hayashi, S. Yamaguchi, H. Shinokubo, *Chem. Eur. J.* **2012**, *18*, 5919.

[10] Y. Matano, T. Shibano, H. Nakano, H. Imahori, *Chem. Eur. J.* **2012**, *18*, 6208.

[11] T. Ito, Y. Hayashi, S. Shimizu, J.-Y. Shin, N. Kobayashi, H. Shinokubo, *Angew. Chem.* **2012**, *124*, 8670; *Angew. Chem. Int. Ed.* **2012**, *51*, 8542.

[12] a) J. L. Sessler, R. S. Zimmerman, C. Bucher, V. Král, B. Andrioletti, *Pure Appl. Chem.* **2001**, *73*, 1041; b) C. Bucher, R. S. Zimmerman, V. Lynch, V. Král, J. L. Sessler, *J. Am. Chem. Soc.* **2001**, *123*, 2099; c) V. Král, J. L. Sessler, R. S. Zimmerman, D. Seidel, V. Lynch, B. Andrioletti, *Angew. Chem.* **2000**, *112*, 1097; *Angew. Chem. Int. Ed.* **2000**, *39*, 1055; d) B. Dolenský, J. Kroulík, V. Král, J. L. Sessler, H. Dvořáková, P. Bouř, M. Bernátková, C. Bucher, V. Lynch, *J. Am. Chem. Soc.* **2004**, *126*, 13714; e) J. M. Benech, L. Bonomo, E. Solari, R. Scopelliti, C. Floriani, *Angew. Chem.* **1999**, *111*, 2107; *Angew. Chem. Int. Ed.* **1999**, *38*, 1957; f) N. Re, L. Bonomo, C. Da Silva, E. Solari, R. Scopelliti, C. Floriani, *Chem. Eur. J.* **2001**, *7*, 2536; g) L. Bonomo, E. Solari, R. Scopelliti, C. Floriani, N. Re, *J. Am. Chem. Soc.* **2000**, *122*, 5312; h) M. O. Senge, S. Runge, M. Speck, K. Ruhlandt-Senge, *Tetrahedron* **2000**, *56*, 8927; i) I. Bischoff, X. Feng, M. O. Senge, *Tetrahedron* **2001**, *57*, 5573.

[13] The ^{1}H NMR spectrum of **2Zn** in $CDCl_3$ displays a highly symmetric feature, which is almost same as free base **2H**, suggesting no dimer formation in the solution state.

[14] The NICS value has been successfully used as a measure of aromaticity, see: a) Z. Chen, C. S. Wannere, C. m. Corminboeuf, R. Puchta, P. v. R. Schleyer, *Chem. Rev.* **2005**, *105*, 3842; b) P. v. R. Schleyer, C. Maerker, A. Dransfeld, H. Jiao, N. J. R. v. E. Hommes, *J. Am. Chem. Soc.* **1996**, *118*, 6317.

[15] H. Ogawa, C. Fukuda, T. Imoto, I. Miyamoto, H. Kato, Y. Taniguchi, *Angew. Chem.* **1983**, *95*, 412; *Angew. Chem. Int. Ed. Engl.* **1983**, *22*, 417.

[16] For sulfur extrusion reactions to afford corrole type structures, see: a) M. J. Broadhurst, R. Grigg, A. W. Johnson, *J. Chem. Soc., Chem. Commun.* **1970**, 807; b) M. J. Broadhurst, R. Grigg, A. W. Johnson, *J. Chem. Soc., Chem. Commun.* **1969**, 23.

[17] S. Zaitseva, S. Zdanovich, O. Koifman, *Russ. J. Coord. Chem.* **2010**, *36*, 323.

[18] a) R. E. Davis, *J. Org. Chem.* **1958**, *23*, 1767; b) N. P. Neureiter, F. G. Bordwell, *J. Am. Chem. Soc.* **1959**, *81*, 578.

[19] The sulfur extrusion reaction of episulfides to alkenes by phosphine proceeds through a one-step mechanism, see: D. B. Denney, M. J. Boskin, *J. Am. Chem. Soc.* **1960**, *82*, 4736.

[20] CCDC-893773 (**2Zn**), CCDC-893772 (**2Ni**), and CCDC-900790 (**2Pt**) contain the supplementary crystallographic data for this paper. These data can be obtained free of charge from The Cambridge Crystallographic Data Centre via www.ccdc.cam.ac.uk/data_request/cif.

Received: September 12, 2012
Published online: November 8, 2012

